Kinetic Studies on the Effect of Yeast Cofilin on Yeast Actin Polymerization[†]

Jinyan Du and Carl Frieden*

Department of Biochemistry and Molecular Biophysics, Box 8231, Washington University School of Medicine, 660 South Euclid Avenue, Saint Louis, Missouri 63110

Received May 13, 1998; Revised Manuscript Received July 10, 1998

ABSTRACT: The effect of yeast cofilin on the kinetics of polymerization of yeast actin has been examined at 20 °C at both pH 8.0 and 6.6. In the absence of cofilin, the kinetic data may be described by a simple nucleation-elongation mechanism. Kinetic data in the presence of cofilin suggests a complex dependence on the cofilin concentration. At low cofilin-to-actin ratios, cofilin increases the rate of polymerization in a way best fit by assuming filament fragmentation. The apparent fragmentation rate constants increase with increasing cofilin concentration leveling off above a cofilin-to-actin ratio of 1:8 and are independent of pH. At higher cofilin-to-actin ratios, a nonpolymerizable cofilin−G-actin complex forms resulting in a decreased rate of polymerization. The data from fluorescence photobleaching recovery experiments at low cofilin-to-actin ratios are consistent with the presence of severed filaments at both pH 8 and 6.6. However, at pH 8 and a cofilin-to-actin ratio of 1:16, about 40−50% of the total actin is present as G-actin after polymerization while at pH 6.6 little or no G-actin is present at the same cofilin-to-actin ratio. The results suggest some cooperativity with respect to cofilin binding to filamentous actin which may be pH dependent.

Actin is one of the major components of the eukayrotic cytoskeleton and its polymerization and depolymerization is tightly regulated by a variety of actin-binding proteins both in vitro (*1*) and in vivo (*2*). In the budding yeast *Saccharomyces cerevisiae*, actin is expressed by a single gene, *ACT1*, that can be easily manipulated by site-directed mutagenesis. Because actin is highly conserved among eukaryotes, yeast actin has become a powerful model for studying actin function as well as the interactions between actin and actin-binding proteins. We previously published data examining the polymerization properties of wild-type yeast actin and a poorly polymerizing yeast actin mutant (R177A/D179A) (*3*). In the course of examining the kinetics of polymerization of yeast actin and other yeast actin mutants, we noted a considerable variability among different wild-type preparations. This variability has now been traced to the presence of a contaminating protein which on further examination was found to be yeast cofilin. Based on this finding, we undertook to examine the role of yeast cofilin on the kinetics of polymerization and depolymerization of yeast actin. Although the effects of proteins from the ADF/cofilin family have been extensively studied, rarely has the cofilin (or ADF) been from the same organism as the actin. Even though actin is highly homologous between yeast and muscle, there still remain differences between the properties of the two proteins. This paper presents data where the proteins both come from yeast and clarifies the role of cofilin in affecting actin polymerization.

Cofilin belongs to a class of proteins, the ADF/cofilin family, that is involved in actin assembly and turnover. Examination of the action of proteins of the ADF/cofilin family on actin polymerization or depolymerization has been reported by a number of investigators [see Moon and Drubin (*4*) for a review] with the general consensus that the primary mechanism of action of these proteins is to sever actin filaments. Carlier et al. (*5*), on the other hand, have recently concluded that dissociation of monomers is the sole mechanism of action and that severing does not occur even though there was a report of direct visual observation of severing activity by actophorin, a member of the ADF/cofilin family (*6*). The view that monomer dissociation is dominant has been challenged by Maciver (*7*), and Theriot (*8*) has suggested that both mechanisms are operative and that distinguishing may require further experimentation. In this paper, we report that the effect of cofilin is complex but that both mechanisms do occur. At low ratios of cofilin to actin, the data are best explained by assuming cofilin binds tightly to and induces fragmentation of filaments with the rate of fragmentation being pH independent. In addition, however, there is a pH-dependent effect such that low cofilin concentrations induce extensive monomer dissociation at pH 8 but not at pH 6.6.

At higher ratios of cofilin to actin, a G-actin−cofilin complex is formed that does not polymerize. Cofilin-induced depolymerization, presumably as a consequence of binding to both F-actin and G-actin, appears to be pH dependent.

MATERIALS AND METHODS

Materials. DNaseI was obtained from Boehringer-Mannheim (Indianapolis) and linked to Affigel 10 (Bio-Rad) as

[†] This work was supported by Grant MCB 9603807 from the National Science Foundation.

* Author to whom correspondence should be sent. Phone: (314) 362-3344. Fax: (314) 362-7183. E-mail: frieden@biochem.wustl.edu.

S0006-2960(98)01117-9 CCC: $15.00
Published on Web 09/02/1998

described by Cook and Rubenstein (*9*). Pyrene-labeled muscle actin was a gift from Drs. J. Cooper and D. Schafer. Rabbit-anti-yeast-cofilin antibody was a gift from Drs. D. Drubin and P. Lappalainen as was the pGEX2T-COF1 plasmid. Cofilin was expressed using this plasmid in JM109 cells and then purified as described by Fedorov et al. (*10*). The cofilin so obtained is not phosphorylated. The GST protein purification module and the ECL reagents were from Amersham Pharmacia Biotech (Piscataway). All other chemicals used were reagent grade.

Purification of Wild-Type Yeast Actin. Wild-type yeast actin was purified from Red Star yeast cake using DNaseI affinity chromatography as previously described by Cook and Rubenstein (*9*) except for a change in the polymerization conditions. Polymerization of actin in the DE52 column fraction pool was initiated by adding 50 mM KCl and 2 mM Mg^{2+}. Any cofilin contamination was removed as described by Yonezawa et al. (*11*). Polymerized actin was incubated at room temperature for 0.5 h, and a concentrated KCl solution was added slowly to a final concentration of 0.8 M. After another 10 min of incubation at room temperature, the filaments were centrifuged at 48K rpm, 4 °C, for 1 h in a Beckman 50Ti rotor. The yield of pure actin (∼5 mg) was not affected by this modification in the protocol.

Western Blotting. About 6 μg of purified yeast actin was loaded into each lane of an SDS gel. Cofilin contamination was detected using the cofilin antibody and a secondary antibody of goat-anti-rabbit-IgG.

Polymerization Assays. Actin polymerization was followed by either the decrease of intrinsic fluorescence (excitation at 300 nm, emission at 335 nm) or the increase of pyrene-labeled muscle actin fluorescence (excitation at 365 nm, emission at 386 nm) at 20 °C. In figures using intrinsic fluorescence, the data have been converted to show an increase as to be comparable to those in which pyrene-labeled actin is used. The reactions were run in a total volume of 200 μL using a PTI (Alphascan) spectrofluorometer. At pH 8.0, the buffer (G8.0) contained 2 mM Tris-Cl, 0.2 mM $CaCl_2$, 0.2 mM ATP, 0.5 mM dithiothreitol, and 0.01% NaN_3. For assays at pH 6.6, the buffer (G6.6) was 10 mM MES, 0.2 mM $CaCl_2$, 0.2 mM ATP, 0.5 mM dithiothreitol, and 0.01% NaN_3. In all cases, the actin was preincubated for 5 min with a Ca^{2+} chelator and a low concentration of Mg^{2+} to replace the tightly bound Ca^{2+} with Mg^{2+}. At pH 8.0, this preincubation was with 1 mM EGTA and 50 μM Mg^{2+}, while at pH 6.6 it was 100 μM BAPTA and 50 μM Mg^{2+}. In experiments where actin filaments were diluted, the dilution was at the same pH as the polymerization (either G8.0 or G6.6).

Simulation of Actin Polymerization. Data fitting utilized more recent versions (*12*) of KINSIM (*13*) and FITSIM (*14*) (KINSIM40 and FITSIM40) that are available from http://www.biochem.wustl.edu/cflab. KINSIM40 was used to simulate an individual data set in order to obtain an approximate fit of the data to the chosen mechanism. FITSIM40 was used to globally fit the data, using the approximations from KINSIM40, as a function of actin concentration at either pH 8.0 or 6.6. Values of 2×10^6 s^{-1} mol^{-1} were used for all on rate constants except for that of the elongation step (step 7) of Scheme 1.

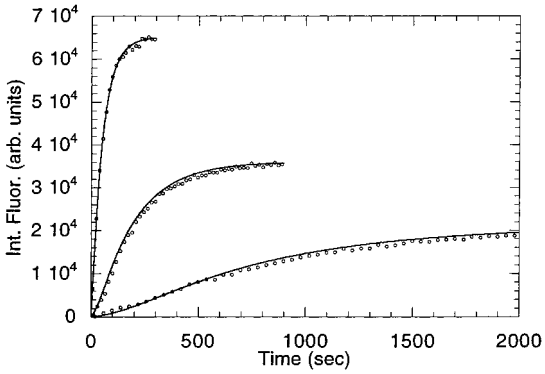

FIGURE 1: Polymerization of cofilin-free yeast actin at pH 8.0 and 20 °C as a function of actin concentration using intrinsic fluorescence as the probe. The polymerization was initiated by the addition of 2 mM Mg^{2+} at pH 8.0 after preincubation to replace tightly bound Ca^{2+} with Mg^{2+} as described in Materials and Methods. The decrease in intrinsic fluorescence with polymerization has been converted to appear as an increase in this and other figures using intrinsic fluorescence. The concentrations of actin used from bottom to top were 5.9 μM (0.25 mg/mL), 11.8 μM (0.5 mg/mL), and 17.7 μM (0.75 mg/mL) and data collected continuously (open symbols). The rate constants used for fitting the data to Scheme 1 (solid lines) were 2 μM^{-1} s^{-1} for $k_3 - k_6$, 0.035 μM^{-1} s^{-1} for k_7, 2 s^{-1} for $k_{-3} - k_{-5}$, 0 for k_{-6}, and 0.001 s^{-1} for k_{-7}. The nucleation dissociation constants for steps 1 and 2 of Scheme 1 are given in Table 1. These values are probably not unique for fitting the data since a unique fit may not be possible to obtain. They are, however, sufficient to represent the characteristics of the mechanism.

Scheme 1

$$A + A \underset{k_{-1}}{\overset{k_1}{\rightleftharpoons}} A_2 \quad (1)$$

$$A_2 + A \underset{k_{-2}}{\overset{k_2}{\rightleftharpoons}} A_3 \quad (2)$$

$$A_3 + A \underset{k_{-3}}{\overset{k_3}{\rightleftharpoons}} A_4 \quad (3)$$

$$A_4 + A \underset{k_{-4}}{\overset{k_4}{\rightleftharpoons}} A_5 \quad (4)$$

$$A_5 + A \underset{k_{-5}}{\overset{k_5}{\rightleftharpoons}} A_6 \quad (5)$$

$$A_6 + A \underset{k_{-6}}{\overset{k_6}{\rightleftharpoons}} A_n \quad (6)$$

$$A_n + A \underset{k_{-7}}{\overset{k_7}{\rightleftharpoons}} A_{n(\text{elongation})} \quad (7)$$

This value was chosen as an approximation of a diffusion controlled association step. The rate constants for step 7 and the reverse of step 2 were allowed to float to give the best fits. Other rate constants are given in the legend to Figure 1. These values are probably not unique for fitting the data but they are internally consistent. For data in the presence of cofilin, KINSIM40 was used with the fitted values and the fragmentation rate constant was varied to give the best fit of the data by eye. As noted in Table 1 it was necessary to change the nucleation dissociation constant slightly to obtain these fits.

Fluorescence Photobleaching Recovery (FPR).[1] FPR experiments were carried out as described previously (*15*) using trace amounts (5−10%) of rhodamine-labeled muscle

Table 1: Parameters for Fitting Data as a Function of Cofilin Concentration

cofilin/actin ratio[a]	relative extent of polymerization	nucleation dissociation constants		fragmentation rate, rate constant (s^{-1})[b]	"free actin"[c] (μM)
		K_1 (μM)	K_2 (μM)		
		pH 8.0			
0	1.0	0.5×10^5	300[d]		5.9
1:64	0.87	0.5×10^5	300	0.004	5.8
1:32	0.79	0.5×10^5	300	0.009	5.7
1:16	0.79	0.5×10^5	100	0.016	5.53
1:8	0.67	0.5×10^5	50	0.028	5.16
1:4	0.58	0.5×10^5	25	0.028	4.42
1:2	0.42	0.5×10^5	100	0.03	2.95
1:1	0.0				0
		pH 6.6			
0	1.0	2.5×10^5	7.5		5.9
1:64	1.0	2.5×10^5	7.5	0.001	5.8
1:32	0.8	2.5×10^5	7.5	0.008	5.7
1:16	0.76	2.5×10^5	7.5	0.016	5.53
1:8	0.74	2.5×10^5	3.5	0.022	5.16
1:4	0.59	2.5×10^5	3.5	0.03	4.42
1:2	0.44	2.5×10^5	3.5	0.027	2.95
1:1	0.0				0

[a] Expertmental conditions: the concentration of actin used was 5.9 μM in all experiments either at pH 8 (G8.0 buffer) or pH 6.6 (G6.6 buffer). Experiments performed as described in legends to Figures 2 and 5, respectively. [b] Values for the reannealing rate constant up to 0.01 s^{-1} have no effect on the simulation. [c] Calculated assuming that the G-actin cofilin complex cannot undergo polymerization. [d] Values for K_1 and K_2 were determined from simulation of the polymerization as a function of actin concentration.

actin, prepared as described elsewhere (*16*), as the fluorophore. For rhodamine, the FPR apparatus used a laser light of 514.5 nm that is focused on a sample via a dichroic mirror in a fluorescence microscope. The sample was bleached with a transient (5 ms) increase in beam intensity of $\sim 10^4$ times the observation beam. The observation beam was of low enough intensity that little photobleaching occurred over the time course of the experiment. For experiments to determine the extent of fragmentation, a 40× objective with a Gaussian beam radius of 1.8 mm was used. Usually 10−20 scans, each at a different spot, were averaged to obtain better signal-to-noise ratios. For experiments to determine the amount of G-actin present, a 4× objective with a Gaussian beam radius of about 15 mm was used. The data were analyzed using the approximate solution (*17, 18*).

$$f(t) = [f(0) + f(\infty)t/\tau_{1/2}]/(1 + t/\tau_{1/2})$$

where $f(0)$ and $f(\infty)$ are the initial and final fluorescent values, and $\tau_{1/2}$ is the recovery time. For slower recovery times, the observation scan time varied between 10 and 40 s, while for the faster recovery times, the observation scan time was between 2 and 4 s. In each case, 1000 points were collected after the bleach and the data were analyzed separately. When the 4× objective was used and there was more than 1 phase of recovery, simulated data comparisons showed that analysis of the faster phase (scan time of 4 s) using the equation above gave approximately correct values for the amount of G-actin relative to total actin present.

RESULTS

A typical protocol for purifying yeast actin has been described by Cook and Rubenstein (*9*). We observed, however, that different preparations gave rather different rates of polymerization under identical experimental conditions. Careful examination of SDS gels of the faster polymerizing preparation indicated varying amounts of a low molecular weight contaminant. Western blots with antibody to cofilin (provided by Drs. Drubin and Lappalainen) showed that this contamination was yeast cofilin. Essentially all of the cofilin contamination could be removed by polymerization with high salt as described in Materials and Methods. After removal, the actin polymerized at a slower rate than previously reported (*3*) and, when using pyrene-labeled actin as the probe for polymerization, showed little overshoot (as shown later) in the time course of polymerization, rather than the relatively large overshoot previously reported (*3*). With cofilin-free actin, we could then examine the effect of yeast cofilin on the kinetics of polymerization. Since it has been reported that cofilin effects are pH dependent (*19, 20*), experiments were performed both at pH 8 and 6.6.

Polymerization of Yeast Actin at pH 8. As previously described (*3, 21*), it is possible to measure actin polymerization using changes in the intrinsic fluorescence of actin. Intrinsic fluorescence measurements, while coincident with the pyrene-labeled measurements, do not show any decrease in the extent of reaction at longer times. Figure 1 shows the time course of polymerization at pH 8 in G8.0 buffer as a function of actin concentration using intrinsic fluorescence as the probe of polymerization. In these, and in all subsequent experiments, the actin was incubated for 5 min in the presence of the Ca^{2+} chelator EDTA and low levels of Mg^{2+} in order to remove Ca^{2+} from the tight binding site and replace it with Mg^{2+} (*22*). This "priming" avoids complications in the kinetics arising from the time dependence of the Mg^{2+} displacing Ca^{2+} at this site (*23*). The solid lines are fits to the data (open symbols) using the minimal mechanism shown in Scheme 1 with rate constants given in the legend to Figure 1 and the nucleation dissociation constants given in Table 1.

In contrast to our earlier interpretation (*3*), the polymerization does not require a filament fragmentation step to fit the data, that step apparently being a consequence of the

[1] Abbreviations: BAPTA, 1,2-bis(2-aminophenoxy)ethane-*N*,*N*,*N*′,*N*′-tetraacetate; FPR, fluorescence photobleaching recovery.

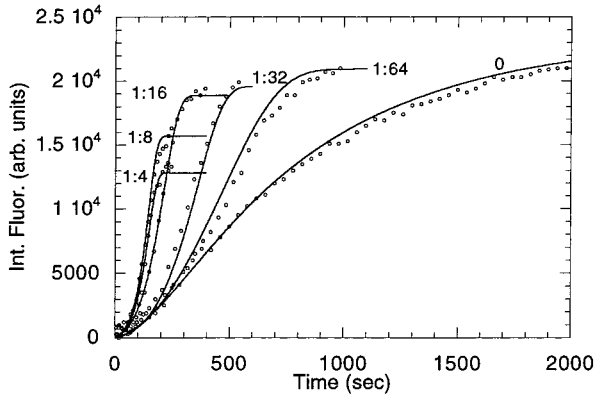

FIGURE 2: Polymerization of yeast actin (0.25 mg/mL, 5.9 μM) as a function of cofilin concentration at pH 8.0 and 20 °C. The time course of polymerization measured using intrinsic fluorescence and the reaction was initiated by the addition of 2 mM Mg^{2+} at pH 8.0 after preincubation to replace tightly bound Ca^{2+} with Mg^{2+} as described in Materials and Methods. The molar cofilin to actin ratios are given in the figure. The symbols represent the fluorescent data (collected continuously) while the solid lines are the fitted data using the values given in Table 1 and in the legend to Figure 1.

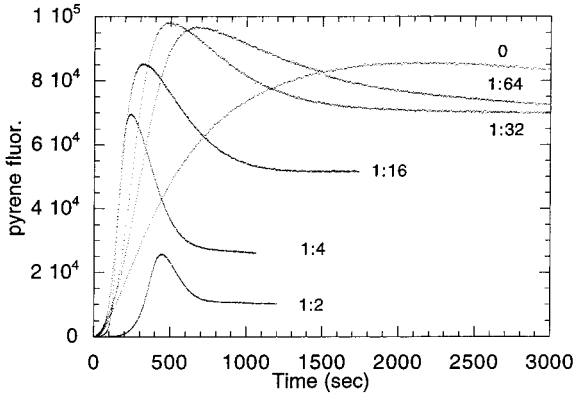

FIGURE 3: Polymerization of yeast actin (0.25 mg/mL, 5.9 μM) as a function of cofilin concentration at pH 8.0 and 20 °C. The time course of polymerization measured using trace amounts of pyrene-labeled actin as the probe and the reaction was initiated by the addition of 2 mM Mg^{2+} at pH 8.0 after preincubation to replace tightly bound Ca^{2+} with Mg^{2+} as described in Materials and Methods. The molar cofilin to actin ratios used are given in the figure.

cofilin contamination in the previous actin preparations. It should be noted that even though the polymerization rate is slower than previously reported, it is still faster than that for muscle actin under identical conditions (data not shown).

Effect of Cofilin on Yeast Actin Polymerization at pH 8. The effect of cofilin on actin polymerization at pH 8 is shown in Figure 2. The data were obtained using intrinsic fluorescence at a single actin concentration (5.9 μM) as a function of cofilin concentration. At all cofilin concentrations shown in this figure, there is a marked increase in the polymerization rate. The increase occurs, however, after a significant lag period, and the lag persists as the ratio of cofilin to actin increases. In order to fit these data, a fragmentation step was added to the mechanism

$$A_n \rightarrow 2A_n \qquad (8)$$

presumably as a consequence of cofilin binding tightly to the F-actin filament. Table 1 lists the rate constants for the fragmentation step as a function of cofilin concentration. At low cofilin-to-actin ratios, the fragmentation rate constant is proportional to cofilin concentration. As the cofilin concentration increases, however, the fragmentation rate constant becomes essentially constant. At higher cofilin concentrations, the lag is shorter and the extent of polymerization is less. At a ratio of 1:1, no polymerization occurs (data not shown).

The solid lines in Figure 2 are the fits to Scheme 1, including the fragmentation step and the constants given in Table 1. To make these fits, we assumed that cofilin bound to G-actin resulted in a nonpolymerizable complex, thereby lowering the total concentration of actin available. This complex formation becomes important only at cofilin-to-actin ratios above 1:8. As shown by Hawkins et al. (*19*), human ADF binds to muscle G-actin with 1:1 stoichiometry at pH 8 sequestering monomers and preventing polymerization. This appears also to be the case for yeast cofilin and yeast actin. On the other hand, the nucleation process appears to be somewhat more effective at higher cofilin concentrations. Either a small amount of the cofilin−G-actin complex may serve to nucleate the polymerization or the complex may have a slight nucleating activity.

When similar experiments are performed using pyrene-labeled actin as the probe for polymerization, data shown in Figure 3 were obtained. As implied from earlier results (*3*) and from the effect of yeast cofilin on muscle actin polymerization (*24*), there is an overshoot in the pyrene fluorescence in the presence of cofilin. (The slight overshoot in the polymerization in the "absence" of cofilin may represent a very small amount remaining in the actin.) The rate and extent of the fluorescence decrease is dependent on the cofilin concentration. Since the pyrene fluorescence increase is associated with incorporation of monomer into filaments (*25, 26*), the decrease may reflect either a dissociation of monomers from the actin filaments with coincident loss of the fluorescence or different fluorescent properties of the filaments produced by fragmentation. The latter is possible since cofilin does induce a different filament twist (*27*). It is also possible, however, that the slow decrease is associated with the hydrolysis of ATP that occurs during polymerization and which may be accelerated by cofilin binding to the filament. Such a conclusion would be consistent with the observation that ADF1 (recombinant ADF from *Arabidopsis thaliana*) increases the rate of ATP hydrolysis in muscle F-actin (*5*).

Polymerization of Yeast Actin at pH 6.6. As with muscle actin (*28*), the rate of yeast actin polymerization increases dramatically with decreasing pH. Figure 4 shows polymerization data as a function of actin concentration at pH 6.6 using changes in the intrinsic fluorescence as the probe of polymerization. In these experiments, Mg^{2+} replacement of Ca^{2+} at the tight-binding site was accomplished by preincubating G-actin with 100 μM BAPTA and 50 μM Mg^{2+} for 5 min prior to addition of Mg^{2+} to promote polymerization. To cover a reasonable range of actin concentrations, the polymerization was performed at a lower Mg^{2+} concentration (1 mM) than was used at pH 8 (2 mM). As shown by the solid lines in the figure the data (open symbols) could be fit by the mechanism given in Scheme 1 without any fragmentation step using the rate constants given in the legend to Figure 1 and the nucleation dissociation constants

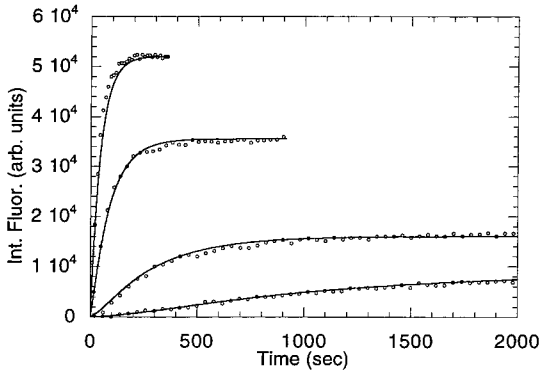

FIGURE 4: Polymerization of cofilin free yeast actin at pH 6.6 and 20 °C as a function of actin concentration using intrinsic fluorescence as the probe. The polymerization was initiated by the addition of 1 mM Mg^{2+} at pH 6.6 after preincubation to replace tightly bound Ca^{2+} with Mg^{2+} as described in Materials and Methods. The concentrations of actin used were from bottom to top 2.95 μM (0.125 mg/mL), 5.9 μM (0.25 mg/mL), 11.8 μM (0.5 mg/mL), and 17.7 μM (0.75 mg/mL). Data collected continuously are shown as open symbols. The rate constants used for fitting the data to Scheme 1 (solid lines) are the same as given in the legend to Figure 1 with the nucleation dissociation constants for steps 1 and 2 given in Table 1.

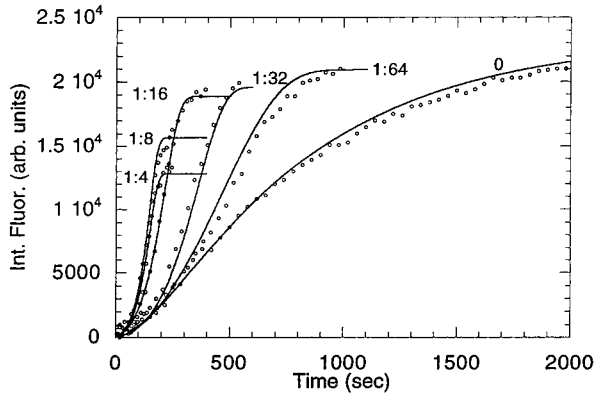

FIGURE 5: Polymerization of yeast actin (0.25 mg/mL, 5.9 μM) as a function of cofilin concentration at pH 6.6 and 20 °C. The time course of polymerization measured using intrinsic fluorescence and the reaction was initiated by the addition of 1 mM Mg^{2+} at pH 6.6 after preincubation to replace tightly bound Ca^{2+} with Mg^{2+} as described in Materials and Methods. The molar cofilin to actin ratios are given in the figure. The symbols represent data collected continuously while the solid lines are the fitted data using the parameters given in the legend to Figure 1 and in Table 1.

given in Table 1. Nucleation parameters, however, differed from those at pH 8 with much more favorable nucleation at pH 6.6, similar to that observed for muscle actin (*28*). We assumed, for simplicity, that the elongation rate was the same at pH 6.6 as at pH 8.

Effect of Cofilin on Yeast Actin Polymerization at pH 6.6. Figure 5 shows the polymerization induced by the addition of 1 mM Mg^{2+} as measured by changes in intrinsic fluorescence at a constant actin concentration (5.9 μM) as a function of cofilin concentration. The solid lines in this figure are fits to the experimental data (symbols) using the parameters listed in Table 1 and the legend to Figure 1. Comparison with similar data at pH 8 (Figure 2) shows relatively similar behavior. At low concentrations, cofilin has little effect on the rate until after a significant lag period. The subsequent increase in rate is consistent, as at pH 8.0, with fragmentation of the filament. When the data are

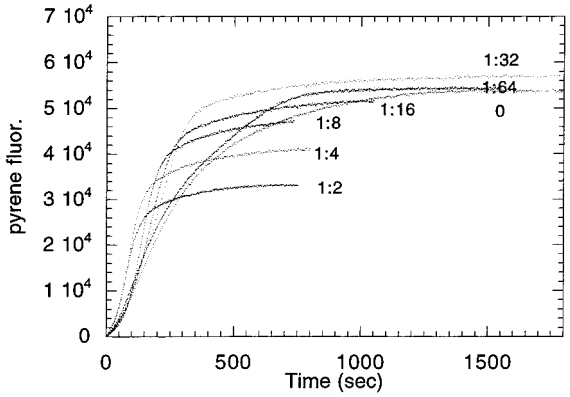

FIGURE 6: Polymerization of yeast actin (0.25 mg/mL, 5.9 μM) as a function of cofilin concentration at pH 6.6 and 20 °C. The time course of polymerization was measured using trace amounts of pyrene-labeled actin and the reaction was initiated by the addition of 1 mM Mg^{2+} at pH 6.6 after preincubation to replace tightly bound Ca^{2+} with Mg^{2+} as described in Materials and Methods. The molar cofilin to actin ratios are given in the figure.

analyzed, including the fragmentation rates, it is found that (except at the lowest cofilin concentration) they are essentially identical to those at pH 8 (Table 1). Thus, the cofilin-induced fragmentation rate constants are independent of pH. In order to fit these data effectively, it is necessary to assume, as was the case at pH 8, that any G-actin−cofilin complex that forms is inactive and decreases the concentration of actin available for polymerization. There also appears to be almost no effect on nucleation as a function of cofilin, suggesting little or no formation of a nucleating species.

Figure 6 shows the polymerization of actin as a function of cofilin under conditions identical to those of Figure 5 except that pyrene-labeled actin is used to measure polymerization. In distinct contrast to similar data obtained at pH 8 (Figure 3) there is no decrease in pyrene fluorescence after the completion of the polymerization process. Interestingly, while the intrinsic fluorescence data indicates no polymerization at a stoichiometry of 1:1 (data not shown), some change in pyrene fluorescence does occur, although after a considerable lag. It is not clear what this represents, although it has been shown that pyrene-labeled G-actin containing ADP has a higher fluorescence than that containing ATP (*29*).

Effect of Cofilin on Depolymerization. If cofilin can fragment filaments, then the rate of depolymerization on dilution should be increased in its presence. Figure 7 shows the effect of a 20-fold dilution (into G-buffer) on the depolymerization of F-actin in the presence and absence of cofilin at either pH 8.0 or 6.6. In this experiment, changes in pyrene-labeled actin (trace amounts) fluorescence were used as the probe of depolymerization and the actin was diluted into depolymerizing buffer at either pH 8.0 (G8.0 buffer) or 6.6 (G6.6 buffer). In both cases, the presence of a substoichiometric amount of cofilin (cofilin:actin ratio of 1:16) increased the rate of depolymerization 6−10-fold with depolymerization at pH 8 being faster than that at pH 6.6 either in the presence or absence of cofilin. Table 2 gives the depolymerization rate constants assuming a simple first-order process for the depolymerization process.

In a somewhat different type of experiment, Carlier et al. (*5*) measured depolymerization with no dilution in the presence of equimolar amounts of DNaseI and excess ADF1

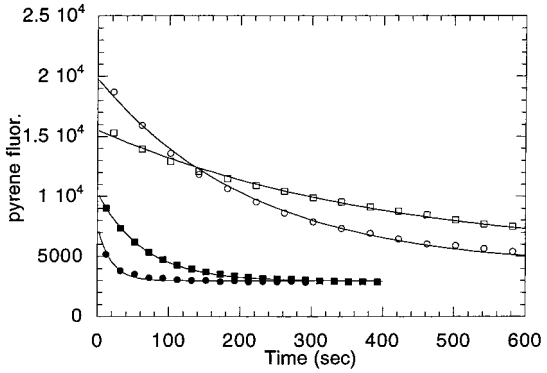

FIGURE 7: Depolymerization of yeast actin on a 20-fold dilution either at pH 8.0 or pH 6.6 in the presence (filled symbols) or absence (open symbols) of cofilin. The actin was polymerized at a concentration of 5.9 μM in the presence or absence of 0.37 μM cofilin (a molar cofilin-to-actin ratio of 1:16) and trace amounts of pyrene-labeled actin until polymerization was complete and then diluted into either pH 8.0, G8.0 buffer (●, ○) or pH 6.6, G6.6 buffer (■, □).

Table 2: Depolymerization Rate Constants (s^{-1}) Measured by Dilution[a]

	−cofilin	+cofilin
pH 8.0	0.0046	0.053
pH 6.6	0.0025	0.015

[a] Experimental conditions: 5.9 μM actin was polymerized in the presence or absence of 0.37 μM cofilin (a molar cofilin to actin ratio of 1:16) and trace amounts of pyrene-labeled actin until polymerization was complete and then diluted into either pH 8.0 G8.0 buffer or pH 6.6 G6.6 buffer. The rate constants were calculated assuming a simple first-order process.

(a member of the cofilin family) concluding that ADF1 did not increase the rate of depolymerization. We therefore measured depolymerization of 6 μM actin in the presence of 6 μM DNaseI without dilution and found that, in contrast to the results of Carlier et al. (*5*), at low cofilin concentrations, the rate of depolymerization was at least 5−10-fold faster than in the absence of cofilin (data not shown).

Fluorescence Photobleaching Recovery. To confirm that shorter filaments are induced by the presence of cofilin, we performed fluorescence photobleaching recovery experiments. Fluorescence photobleaching recovery (FPR) measures the diffusion of a fluorescently labeled molecule into a spot previously bleached by a high intensity laser beam. As has been shown elsewhere (*15*), actin molecules become immobile as polymerization proceeds presumably as a result of network formation. To test the effect of cofilin on actin filaments, FPR experiments were performed as a function of cofilin concentration and the recovery times measured after polymerization had been completed. The time of recovery, t_d, is related to the diffusion coefficient by

$$t_d = \omega^2/4D$$

where ω is the Gaussian beam radius. Figure 8 shows data obtained at pH 8.0 using 23 μM (1 mg/mL actin) polymerized with 2 mM Mg^{2+} at different concentrations of cofilin. In the absence of cofilin, yeast actin is immobilized similar to the results previously observed for muscle actin (*15*). At very low molar ratios of cofilin to actin (1:64), actin filaments become mobile, suggesting that the filaments are being severed by cofilin, although at this cofilin-to-actin ratio, the shape of the recovery curve is not typical of normal recovery. As the concentration of cofilin is increased, the recovery times decrease, indicating more extensive fragmentation. In all cases, the final fluorescence has reached the prebleach value (shown as the first 10% of the plot) showing that the filaments are completely mobile. Close examination of Figure 8 suggests a minimum of two processes, one that becomes faster with increasing cofilin concentration and one that is quite rapid being completed in less than 1 s. The recovery times of the filaments produced by the slower process decrease as the cofilin concentration increases and are given in the legend to Figure 8. The faster process is not well determined in these experiments, and to clarify the nature of the rapid phase, similar FPR experiments were performed using a larger (4×) objective for which recovery times should be about 100-fold slower than with the 40× objective. In this case, G-actin alone has a recovery time of 1.2 s (data not shown). Figure 9 shows an FPR experiment for a cofilin-to-actin ratio of 1:16 (actin = 23 μM, cofilin = 1.45 μM) at both pH 8.0 and 6.6 clearly demonstrating the difference in recovery times at the two pH values. At pH 8.0, the fast phase (seen in Figure 9B) accounts for about half the total actin present (seen in Figure 9A) and has the recovery time of G-actin itself. By 90 s, there has not been complete recovery, indicating longer filaments. Data at the same cofilin-to-actin ratio but using the 40× objective shows that these filaments are mobile (Figure 8, 1:16). At pH 6.6, there is little, if any, fast phase with a recovery time of G-actin. Rather, there is a single phase with almost complete recovery by 90 s. The recovery time for this phase is 40 s. Assuming that the filaments are rodlike, a mean length of about 2 mm (about 800 subunits) can be calculated from the theory of Garcia de la Torre and Bloomfield (*30*). This must be interpreted to mean that, at this cofilin-to-actin ratio (1:16), an appreciable amount of G-actin is present at pH 8.0 after polymerization has been completed, but little or no G-actin is present at the lower pH. This difference may explain the pH dependence of the effect of cofilin on actin polymerization.

DISCUSSION

As noted earlier, we found that different preparations of yeast actin gave rather different rates of polymerization under the same experimental conditions. Specifically, later preparations polymerized at rates slower than those previously published (*3*). The reason for these differences was found to be a consequence of different amounts of yeast cofilin present as a contaminating protein in different preparations. This is disturbing because most investigators use the same method of preparation of yeast actin as originally described by Cook and Rubenstein (*9*). After cofilin was removed from the yeast actin, we reexamined the kinetics of actin polymerization as a function of actin concentration and found, in contrast to previous conclusions (*3*, *31*), that filament fragmentation of yeast actin was not a factor in the polymerization process in the absence of cofilin. That is, the data shown in Figures 1 and 4 could be easily fit by the mechanism shown in Scheme 1 without assuming fragmentation. Since these results were different from those previously published, we turned to the investigation of effect of cofilin on polymerization. Although such effects have been

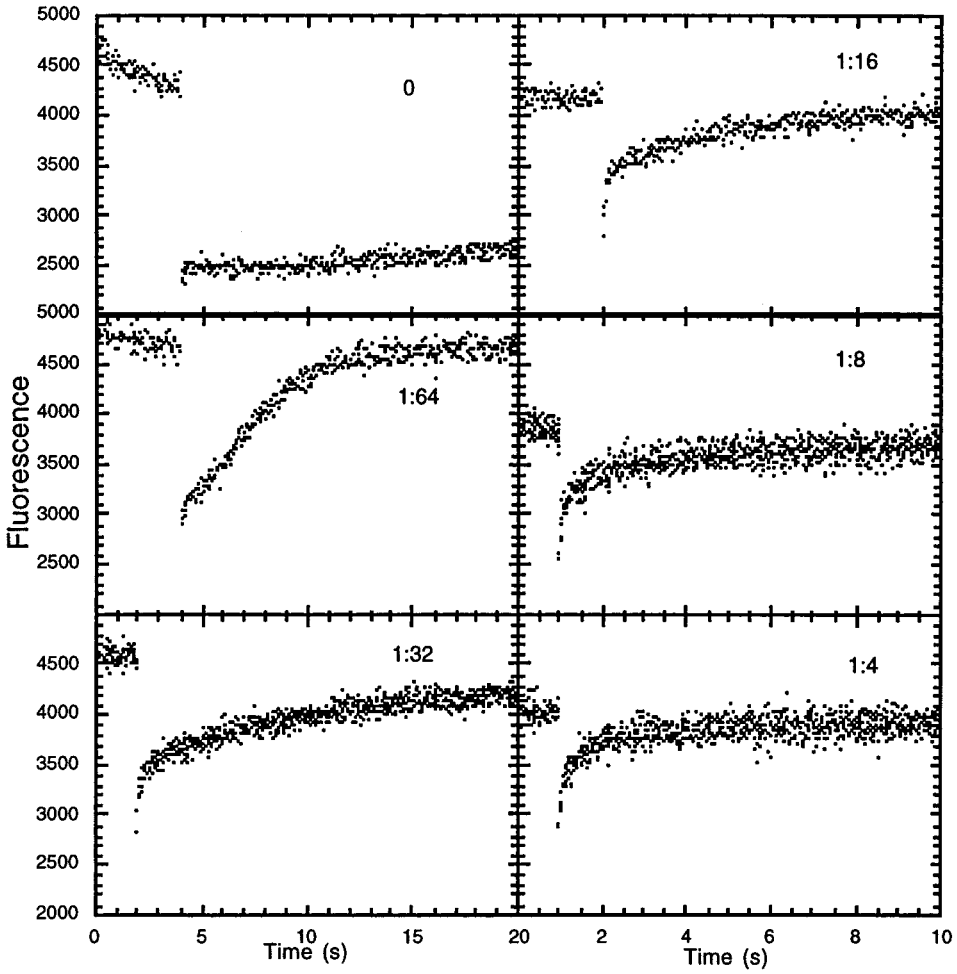

FIGURE 8: Recovery of actin polymerized in the absence or presence of cofilin using fluorescence photobleaching recovery (FPR) as the measure of diffusion. Experiments were performed by polymerizing actin with a trace amount of rhodamine-labeled actin at pH 8 for approximately 30 min before measurements were taken. The actin concentration used was 23 μM (1 mg/mL) and the molar cofilin-to-actin ratios are given in the figure. Recovery times for the major slow process are calculated as 8 s (1:32), 2.3 s (1:16), 1.1 s (1:8), and 0.6 s (1:4). Note that the total time for the experimental data on the left side of the plot is 20 s while that on the right side is 10 s. Other experimental details are given in Materials and Methods.

examined by a number of investigators most studies on the polymerization or depolymerizaton of actin have used actin and cofilin/ADF proteins from different sources. In this investigation, both the actin and cofilin are from yeast, and therefore the effects might be expected to more closely mimic the in vivo situation or at least be more relevant to the interactions that may occur in vivo.

The kinetic data presented here show (1) that there is a complex effect of cofilin on actin polymerization and (2) a pH dependence of release of G-actin from filaments in the presence of cofilin. At either pH 8 or 6.6 and low cofilin-to-actin ratios, the polymerization rate increases only after a cofilin-independent lag period. At higher cofilin concentrations, approaching stoichiometric, there is a long lag period, and at a 1:1 ratio of cofilin-to-actin, polymerization does not occur. In describing the effect of cofilin on actin polymerization, we found that it was not possible at this time to write a specific mechanism that would explain the results on polymerization as a function of cofilin concentration. It was possible, however, to satisfactorily fit the data at the lower cofilin concentrations by assuming that there is fragmentation of the filaments and that the fragmentation step is dependent on cofilin concentration. Interestingly, the rate constant for the fragmentation step levels off at high cofilin concentrations, and the fragmentation rate constants are essentially the same at both pH 6.6 and 8.0 (Table 1). The saturation behavior of the rate constant may reflect cooperativity with respect to binding and the corresponding change in the filament twist (*27*). To fit the polymerization data at the higher cofilin-to-actin ratios, however, it was necessary to make two more assumptions. The first is that cofilin binds to G-actin and that this complex cannot undergo polymerization. Such an interaction has been demonstrated for ADF (*19*, *32*, *33*). The second, somewhat more speculative assumption is that either a small proportion (less than 0.1%) of the G-actin−cofilin complex may serve as a nucleating species or that the complex itself has a low nucleating activity. This assumption arises from the small changes in nucleation steps needed for data fitting (see Table 1).

There is evidence both for (*7*, *19*, *34*, *35*) and against (*5*) cofilin-induced fragmentation. Although Carlier et al. (*5*) have presented evidence that ADF1 increases the rate of treadmilling by increasing dissociation of subunits from the pointed end of the filament, we have not been able to construct a mechanism that incorporates just these steps and can still fit the data as a function of cofilin concentration. Fluorescence photobleaching recovery experiments clearly

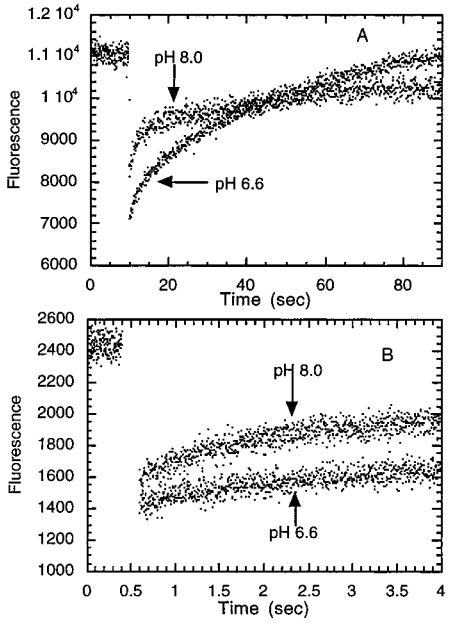

FIGURE 9: FPR experiments at pH 8.0 (G8.0 buffer) and 6.6 (G6.6 buffer). Actin was polymerized at 22 °C for 30 min in the presence of 1 mM Mg^{2+} at either pH and FPR measurements made with a scan time of 90 s (A) or 4 s (B) using a 4× objective. At both pH values polymerization was complete. The actin concentration used was 23 μM (1 mg/mL) and the molar cofilin-to-actin ratio was 1:16.

show that low levels of cofilin result in shorter actin filaments and the kinetic data of Figures 2 and 5 are most consistent with filament fragmentation.

It is of interest to examine more closely the data shown in Figures 8 and 9. First, as shown elsewhere (*15*), and here for the yeast protein (Figure 8), actin becomes immobile as a consequence of polymerization. This has been interpreted to mean that there is formation of a network of actin filaments probably related to the high viscosity observed in nonperturbed actin solutions (*15*). At the lowest cofilin concentration used (cofilin-to-actin ratio 1:64), the filaments become mobile but the shape of the curve reflects some movement of the bleached spot with time implying some disruption of network. As the concentration of cofilin increased, however, the filaments become completely mobile and there are at least two recovery times observed. The slower of the two is probably too slow to represent a single species rather being some type of partial network, i.e., smaller groups of noncovalently associated filaments. For example, a recovery time of 8 s (corresponding to a diffusion coefficient of 1×10^{-9} cm^2 s^{-1}) is observed at a ratio of cofilin to actin of 1:32 (Figure 8). This would correspond, for a cylinder (*30*), to a filament length of about 80 mm (about 30 000 subunits) which seems unreasonable. At a cofilin-to-actin ratio of 1:16, that used for the data shown in Figure 9, the filament length would be about 10 mm. There are two points to consider. First, if the mechanism of cofilin action is simply filament shortening, this would imply an increase of G-actin concentration on the order of 85%. To detect the presence of G-actin, FPR experiments were performed with a microscope objective that decreases the observed recovery times by about 100-fold. The data obtained at pH 8.0 (Figure 9), collected at a cofilin-to-actin ratio of 1:16, shows 40−50% of the total actin is in the form of G-actin with a slower component. At pH 6.6, on the other hand, there is essentially no G-actin present at this cofilin-to-actin ratio. Instead, there is a mobile phase corresponding to a filament size of about 2 mm consisting of about 800 subunits, shorter than that observed at pH 8 using the same cofilin-to-actin ratio. Thus, it appears that cofilin-induced release of G-actin from actin filaments is strongly pH dependent. In this experiment, the concentration of G-actin present at pH 8 at the completion of the polymerization (∼10 μM, about 40−50% of the total actin) is much larger than the cofilin concentration used (1.4 μM). Second, the filaments are much longer than would expected for a random severing process. If cofilin were similar to gelsolin, for example, one would expect rather short filaments at cofilin-to-actin ratios greater than 1:32. Both of these points indicate that the cofilin binding to filamentous actin is cooperative and that the cooperativity may be pH dependent.

Cofilin and cofilin-like proteins have been shown to exhibit a pH-dependent control of actin polymerization (*19*, *20*, *33*). The pH-dependent effects of cofilin may be related to the pH dependence of actin polymerization, to the extent of fragmentation or to the amount of G-actin induced by the presence of cofilin. Hawkins et al. (*19*) have observed a pH dependence of human ADF binding to muscle actin, binding occurring at pH 6.6 but not at pH 8.0 and proposed a pH sensitive cofilin-induced destruction of actin filaments. Yeast cofilin appears to bind well to yeast actin at both pH 8 and 6.6 since strong cofilin effects are observed at both pH values. On the other hand, cofilin-induced depolymerization is pH sensitive, being faster at pH 8.0 than at pH 6.6 (Figure 7 and Table 2).

Figure 7 shows that cofilin markedly increases the rate of depolymerization of actin in contrast to the data presented by Carlier (*5*). This figure also shows that depolymerization is faster at pH 8.0 than at pH 6.6, reinforcing the idea that the effect of cofilin is pH dependent.

Finally, it has been noted here and elsewhere (*3*) that when pyrene-labeled actin is used as a probe of polymerization, there is an apparent overshoot in the fluorescence. We now know that this behavior is a consequence of the presence of cofilin as shown here (Figure 3) as also demonstrated by Moon et al. using muscle actin (*24*). Comparison of the intrinsic fluorescence data and data obtained with pyrene-labeled actin (compare Figures 2 and 3) show that the decrease in fluorescence occurs only after polymerization is complete. A similar overshoot phenomenon is not observed at pH 6.6. While it is still not clear what this overshoot represents, one can model this decrease at pH 8 by assuming dissociation of a species from the filament with a high critical concentration or filaments with a lower fluorescence. McGough et al. (*27*) noted dramatic differences in appearance of cofilin labeled filaments in cryomicrographs at pH 6.6 and 8 with the latter forming bundles of short filaments. It should be noted in this regard that while polymerization measured using pyrene-labeled actin or intrinsic fluorescence track together well at pH 8.0, some differences are seen at pH 6.6 (data not shown).

ACKNOWLEDGMENT

We thank Drs. J. Cooper, E. Elson, and J. Buzan for helpful discussions, Drs. D. Drubin and P. Lappalainen for the cofilin plasmid and antibody, and W. McConnaughey and E. Elson for help with the FPR instrumentation.

REFERENCES

1. Pollard, T. D., and Cooper, J. A. (1986) *Annu. Rev. Biochem. 55*, 987−1035.
2. Drubin, D. G. (1990) *Cell Motil. Cytoskeleton 15*, 7−11.
3. Buzan, J. M., and Frieden, C. (1996) *Proc. Natl. Acad. Sci. U.S.A. 93*, 91−95.
4. Moon, A., and Drubin, D. G. (1995) *Mol. Biol. Cell 6*, 1423−1431.
5. Carlier, M. F., Laurent, V., Santolini, J., Melki, R., Didry, D., Xia, G. X., Hong, Y., Chua, N. H., and Pantaloni, D. (1997) *J. Cell Biol. 136*, 1307−1322.
6. Maciver, S. K., Zot, H. G., and Pollard, T. D. (1991) *J. Cell Biol. 115*, 1611−1620.
7. Maciver, S. K. (1998) *Curr. Opin. Cell Biol. 10*, 140−144.
8. Theriot, J. A. (1997) *J. Cell Biol. 136*, 1165−1168.
9. Cook, R. K., and Rubenstein, P. A. (1992) *The generation of actin mutants* (Carraway, K. L. and Carraway, C. A. C.. Eds) pp 99−122, Oxford Press, New York.
10. Fedorov, A. A., Lappalainen, P., Fedorov, E. V., Drubin, D. G., and Almo, S. C. (1997) *Nat. Struct. Biol. 4*, 366−369.
11. Yonezawa, N., Nishida, E., Maekawa, S., and Sakai, H. (1988) *Biochem. J. 251*, 121−127.
12. Dang, Q., and Frieden, C. (1997) *Trends Biochem. Sci. 22*, 317.
13. Barshop, B. A., Wrenn, R. F., and Frieden, C. (1983) *Anal. Biochem. 130*, 134−145.
14. Zimmerle, C. T., and Frieden, C. (1989) *Biochem. J. 258*, 381−387.
15. Tait, J. F., and Frieden, C. (1982) *Biochemistry 21*, 3666−3674.
16. Tait, J. F., and Frieden, C. (1982) *Biochemistry 21*, 6046−6053.
17. Yguerabide, J., Schmidt, J. A., and Yguerabide, E. E. (1982) *Biophys. J. 40*, 69−75.
18. Petersen, N. O., Felder, S., and Elson, E. L. (1986) in *Handbook of Experimental Immunology* (Weir, D. M., Ed.) pp 24.1−24.23, Blackwell Scientific Publications, Oxford.
19. Hawkins, M., Pope, B., Maciver, S. K., and Weeds, A. G. (1993) *Biochemistry 32*, 9985−9993.
20. Yonezawa, N., Nishida, E., and Sakai, H. (1985) *J. Biol. Chem. 260*, 14410−14412.
21. Selden, L. A., Kinosian, H. J., Estes, J. E., and Gershman, L. C. (1994) *Adv. Exp. Med. Biol. 358*, 51−57.
22. Zimmerle, C. T., Patane, K., and Frieden, C. (1987) *Biochemistry 26*, 6545−6552.
23. Frieden, C. (1983) *Proc. Natl. Acad. Sci. U.S.A. 80*, 6513−6517.
24. Moon, A. L., Janmey, P. A., Louie, K. A., and Drubin, D. G. (1993) *J. Cell. Biol. 120*, 421−435.
25. Tellam, R., and Frieden, C. (1982) *Biochemistry 21*, 3207−3214.
26. Cooper, J. A., Walker, S. B., and Pollard, T. D. (1983) *J. Muscle Res. Cell Motil. 4*, 253−262.
27. McGough, A., Pope, B., Chiu, W., and Weeds, A. (1997) *J. Cell Biol. 138*, 771−781.
28. Zimmerle, C. T., and Frieden, C. (1988) *Biochemistry 27*, 7766−7772.
29. Pantaloni, D., Carlier, M.-F., Coue, M., Lal, A. A., Brenner, S. L., and Korn, E. D. (1984) *J. Biol. Chem. 259*, 6274−6283.
30. Garcia de la Torre, J. G., and Bloomfield, V. A. (1981) *Q. Rev. Biophys. 14*, 81−139.
31. Kim, E., Miller, C. J., and Reisler, E. (1996) *Biochemistry 35*, 16566−16572.
32. Giuliano, K. A., Khatib, F. A., Hayden, S. M., Daoud, E. W., Adams, M. E., Amorese, D. A., Bernstein, B. W., and Bamburg, J. R. (1988) *Biochemistry 27*, 8931−8938.
33. Hayden, S. M., Miller, P. S., Brauweiler, A., and Bamburg, J. R. (1993) *Biochemistry 32*, 9994−10004.
34. Harris, H. E., and Weeds, A. G. (1983) *Biochemistry 22*, 2728−2741.
35. Nishida, E. (1985) *Biochemistry 24*, 1160−1164.

BI981117R